

# Analytical Characterization of the Blockage Process in 3GPP New Radio Systems with Trilateral Mobility and Multi-connectivity

Dmitri Moltchanov\*, Aleksandr Ometov, Yevgeni Koucharyavy

*Tampere University of Technology, Tampere, Finland*

---

## Abstract

One of the recent major steps towards 5G cellular systems is standardization of 5G New Radio (NR) operating in the millimeter wave (mmWave) frequency band. This radio access technology (RAT) will potentially provide extraordinary rates at the access interface enabling the set of new bandwidth-greedy applications. However, the blockage of the line-of-sight (LoS) path between 3GPP NR access point (AP) and the user equipment (UE) is known to drastically degrade the performance of the NR communication links thus leading to potential outage conditions. Although the problem of characterizing LoS blockage process has been addressed in the recent literature, the proposed models are mostly limited to stationary locations of APs and UE. In our study, we characterize properties of the LoS blockage process under simultaneous mobility of both blockers and UE. The model is then extended to the cases of Poisson AP deployment, multi-connectivity, and mobility of AP representing ‘trilateral’ (three-sided) mobility model. We also specify a Markov-based model of the blockage process that can be efficiently used in both system level simulations and analytical analysis of 3GPP NR systems. Using this model we demonstrate how to derive various metrics of interest including (i) fraction of time in blockage, (ii) SNR and capacity process dynamics, (iii) probability that at time  $t$  UE is at the blockage or non-blockage state, (iv) mean and distribution of time to an outage.

*Keywords:* 3GPP New Radio, mmWave, LoS blockage dynamics, mobility, Markov model

---

## 1. Introduction

One of the effective ways to satisfy continually growing user traffic demands is to move higher in the frequency band from microwaves to millimeter waves (mmWave, 30–300GHz) [1, 2, 3], and further to terahertz (THz, 0.3–3THz) band [4], where significant portions of the spectrum are still available. Responding to these trends, 3GPP has recently completed a standalone standardization of the NR technology operating in lower frequencies of the mmWave band. While vendors and network operators are currently performing field trials of this new wireless access technology, research continues their efforts on fine tuning of NR systems making them applicable to various communications scenarios and use-cases [5, 6, 7].

The 3GPP NR systems are expected to be deployed in indoor open spaces and outdoor environments, such

as halls, lobbies, squares, crossroads, parks among others [8, 9, 10]. One of the distinguishing features of communications systems operating in mmWave band is the propagation paths blockage by the relatively small dynamic objects, such as human bodies, vehicles, etc. Fundamentally, as electromagnetic waves cannot “travel around” the objects whose size is smaller than their wavelengths – the human bodies serve as absorbers for the line-of-sight (LoS) propagation path [11]. Thus, to understand and describe the performance regimes of NR systems, it is essential to characterize the LoS blockage dynamics.

As there is an extreme difference in the received signal strength in LoS blocked and LoS non-blocked conditions, blockage of LoS frequently leads to outages [12, 13, 14]. To combat these consequences, 3GPP has recently proposed the concept of multi-connectivity. According to it, UE is allowed to maintain the links to several APs and dynamically switch between them in case of outages. It has been recently demonstrated that this technique might substantially improve various UE-centric metrics including both fraction of time in outage and throughput [15, 16, 17].

Many studies have addressed the problem of LoS blockage modeling. The first class of models characterizes blockage properties when both UE and AP are stationary. The authors in [18] consider infinitesimal and point receivers associated with UE in a field of stationary human block-

---

\*Corresponding Author.

*Email addresses:* [dmitri.moltchanov@tut.fi](mailto:dmitri.moltchanov@tut.fi) (Dmitri Moltchanov), [aleksandr.ometov@tut.fi](mailto:aleksandr.ometov@tut.fi) (Aleksandr Ometov), [evgeni.kucheryavy@tut.fi](mailto:evgeni.kucheryavy@tut.fi) (Yevgeni Koucharyavy)

This paper is an extended version of work “On the Fraction of LoS Blockage Time in mmWave Systems with Mobile Users and Blockers” presented at the 16th International Conference on Wired/Wireless Internet Communications (IFIP WWIC 2018).

ers represented by cylinders. In these settings, the LoS blockage is fully characterized by a single metric – LoS blockage probability. The blockage probability has been shown to increase exponentially with distance. Similar results have been reported in [19, 20] for different shapes of blockers. Several studies address the case of mobile UEs in a field of stationary blockers. In this class of models, the LoS state of UE changes in time forming a stochastic process. Particularly, the authors in [21] derived conditional probability of the UE being in blocked/non-blocked state at time  $t + \Delta t$ ,  $\Delta t > 0$  given that UE has been in blocked/non-blocked state at time  $t$  partially characterizing the LoS blockage process. The temporal effects caused by the blockers mobility around stationary UE have been studied in [22]. The authors have shown that the stochastic properties of the LoS blockage process heavily depends on UEs and blockers mobility parameters.

In many practical communications scenarios, UE and blockers are both mobile. Despite significant efforts invested to date, only little is known about the blockage process with mobile blockers and UE. The underlying reason is that the probabilistic characteristics of the LoS blockage process may vary in time requiring complex models and associated techniques to characterize this dependence analytically. On the other hand, performance assessment of NR deployments in system level simulations (SLS) is a time-consuming task due to the need for tracking not only locations of UEs but blockers as well [22]. Finally, modern and future use-cases are likely to feature the mobile access points, e.g., aerial APs based on the unmanned aerial vehicles (UAVs) [23, 24], vehicular APs mounted on cars, naturally leading to even more complex trilateral (three-sided) mobility scenarios.

Following our previous work [25], this paper aims to propose a model for LoS blockage process when UE and blockers are both mobile. We characterize LoS blockage process characteristics including the fraction of time LoS is available and time intervals UE spends in LoS blocked and non-blocked conditions. We then extend the baseline model to the cases of homogeneous Poisson deployment of APs, AP mobility, and multi-connectivity operation. The resulting model is represented by an inhomogeneous Markov chain whose transition intensities are explicit functions of environmental variables. The Markov representation allows not only for usage of the developed model in SLS studies of 3GPP NR technology but for analytical solutions for a wide range of metrics of interest including (i) SNR and capacity process characteristics, (ii) probability that at time  $t$  UE is at the blockage or non-blockage state, and (iii) fraction of time in blockage and (iv) mean and distribution of time to outage.

The main contributions of our study are:

- Characterization of the LoS blockage process properties including a fraction of time LoS is available between AP and UE and time intervals UE spends in LoS blocked and LoS non-blocked states when UE

and blockers are both mobile;

- Formalization of the simple Markov model capturing basic properties of the LoS blockage process suitable for both SLS and analytical performance assessment of NR technology;
- Extension of the baseline model to various NR specifics and use-cases including 3GPP multi-connectivity option, mobile APs, random AP deployments, arbitrary trajectories of UE, and random UE mobility.

The rest of the paper is organized as follows. Section 2 introduces the system model. Next, we characterize the LoS blockage process and formalize its Markov model in Section 3. Section 4 provides a set of the model extensions. Further, Section 5 gives an overview of feasible applications. Section 6 provides numerical results. Conclusions are drawn in the last section.

## 2. System Model

In our study, we first focus on both conventional infrastructure-based case, where AP serves the tagged user and the remaining ones act as potential blockers, and D2D scenario, where two UEs form a direct link between each other but other users could block it. The height of the AP is constant and is set equal to  $h_A$ . The corresponding communications modes are illustrated in Fig. 2 while notation is provided in Table 1.

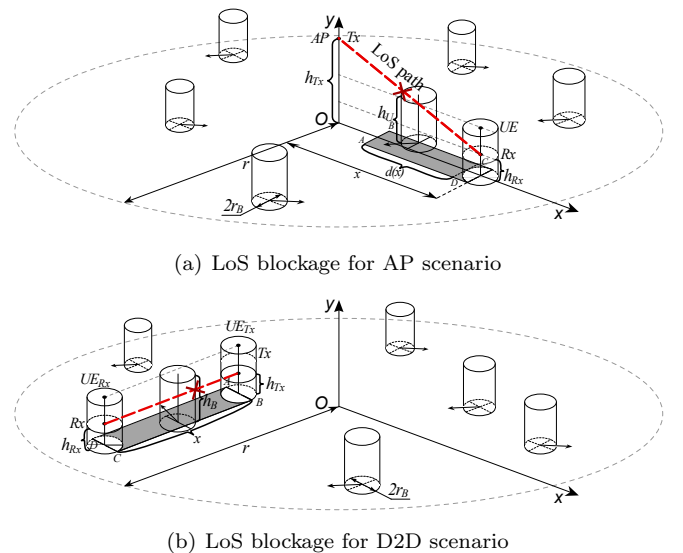


Figure 1: Considered scenarios with mobile UE and blockers.

UEs are assumed to be associated with humans or other entities carrying communications equipment. Communications entities acts as blockers to LoS propagation path and are modeled by *cylinders* with constant base radius  $r_B$  and height  $h_B$ . The height of the UE is constant

Table 1: Main notation used in this paper.

Notation	Details
$\lambda_A$	AP spatial density per $\text{m}^2$
$\lambda_B$	Blocker spatial density per $\text{m}^2$
$h_{Rx}$	UE height, m
$h_{Tx}$	Transmitter height, m
$h_A$	AP height, m
$h_B$	Blocker height, m
$h_U$	UE height, m
$r_B$	Blocker base radius, m
$v_B$	Blocker speed, m/s
$v_U$	UE speed, m/s
$\tau$	Mean blocker movement duration in RDM, s
$K$	Degree of multiconnectivity
$N$	Number of blockers
$w_U(t)$	Trajectory of a moving UE
$w_A(t)$	Trajectory of a moving AP
$g(t)$	Distance between AP and UE at time $t$
$G$	Distance between AP and UE at time $t_0$
$\alpha, \beta$	Intensity of blocked and non-blocked intervals, 1/s
$\delta(\cdot)$	Kronecker delta function
$\gamma$	Intensity of blockers entering LoS blockage zone
$(\vec{\rho}, S)$	Phase-type distribution representation
$\Theta, \Omega$	Blocked and non-blocked period durations
$R_O$	AP radius without outage, m
$p_B, p_L$	Blockage and non-blockage probabilities
$p_i(t)$	Probability of state $i$ at time $t$
$p_{L,i}$	LoS probability with $i - s$ AP
$C(t)$	Time-dependent Shannon capacity, bits/s
$S(t)$	Time-dependent SNR at time $t$ , dB
$S_O$	SNR reception threshold
$S_B$	Area of LoS blockage zone, $\text{m}^2$
$x$	Distance between AP and UE, m
$[x_i(t), y_i(t)]$	Time-dependent UE coordinates
$B$	Bandwidth, Hz
$c$	Constant accounting for imperfection of MCSs
$P_T$	Transmit power, W
$G_T, G_R$	Linear transmit and receive antenna gains
$N_F$	Noise level at bandwidth $B$ , W
$f_X(x)$	Probability density function of $X$
$F_X(x)$	Cumulative distribution function of $X$

$h_U, h_U < h_B$ . Centers of cylinders are assumed to follow the Poisson process in  $\mathbb{R}^2$  with the spatial intensity of  $\lambda_B$  blockers per square meter.

To capture blocked/non-blocked dynamics, we assume that the obstacles move according to random direction model (RDM, [26]) since it captures the essentials of random movement and still allows for analytical tractability. According to this model, a blocker first randomly chooses the direction of movement uniformly in  $(0, 2\pi)$  and then moves in this direction at constant speed  $v_B$  for exponentially distributed time with parameter  $\mu = 1/E[\tau]$ , where  $\tau$  is the mean movement duration. The process is restarted at the stopping point. Whenever blockers cross the LoS

path between the tagged user and NR AP, the LoS is assumed to be blocked. As the user movement is random, and there could be more than a single user blocking LoS, the non-blocked and blocked time intervals are random variables (RV).

To capture the effects of the multi-connectivity operation of NR systems we then extend the single AP deployment to the case of homogeneous Poisson point process deployment of APs and blockers with intensities  $\lambda_A$  and  $\lambda_B$ , respectively. In this deployment, we consider various types of UE mobility. The baseline model assumes that UE with an active session moves along a deterministic trajectory,  $w_U(x) = ab + x$ , at constant speed  $v_U$ . The height of the UE is  $h_U$ . Besides, we assume that UE may also move according to RDM.

### 3. Blockage Characterization and Modeling

In this section, we analyze the baseline UE blockage process with mobile UE and blockers. We first derive the fraction of time UE is in LoS conditions and then proceed characterizing blockage and non-blockage time intervals. Finally, we formulate the Markov LoS blockage model capturing essentials of the LoS blockage process.

#### 3.1. LoS Blockage Fraction

Consider first, the LoS blockage fraction. Here, we assume that UE moves according to RDM in a coverage zone as illustrated in Fig. 2.

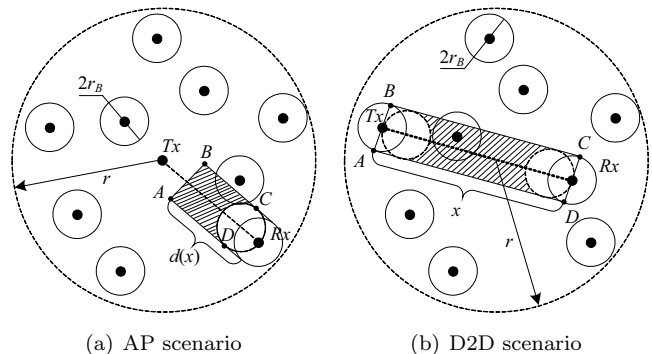


Figure 2: Top view of the LoS blockage zone.

##### 3.1.1. AP Scenario

Let UE be located at the distance  $x$  from the AP at time  $t$ . The LoS to the UE could be blocked by the blockers that are located in the so-called *LoS blockage zone*, marked in gray. The length of this zone is

$$d(x) = \frac{x(h_B - h_{Rx})}{h_{Tx} - h_{Rx}}. \quad (1)$$

Observing the top view of the scenario, Fig. 2(a), note that the area of the LoS blockage is more complicated than

a rectangle. To prevent overlapping, a blocker cannot be located closer than at  $2r_B$  to the user. The area of the LoS blockage zone is then

$$S_B = 2r_B[x - d(x)] - 2r_B^2 - \frac{1}{2}\pi r_B^2. \quad (2)$$

The existence of the zone around the UE prohibiting the presence of blockers implies that the minimum distance from the AP results in non-zero LoS blockage zone is  $2r_B$ . Recall that the limiting RDM distribution is uniform over the area of interest [26]. Observing the system in stationary regime, the probability of a point uniformly distributed in the circle ‘hitting’ a LoS blockage area is given by the ratio  $S_B/\pi r^2$ . Generalizing to  $N$  blockers, we arrive at

$$p_B = 1 - \left(1 - \frac{2r_B[x - d(x)] - 2r_B^2 - \frac{1}{2}\pi r_B^2}{\pi r^2}\right)^N. \quad (3)$$

The probability density function (pdf) from a center of the circle with radius  $r$  to a point uniformly distributed in this circle is given by  $f(x) = 2x/r^2$  [27]. Thus, the probability of having LoS at a random moment of time,  $p_L$ , coinciding with the fraction of LoS, is

$$p_L = 1 - \int_{2r_B}^r \frac{2x \left[1 - \left[1 - \frac{2r_B[x - d(x)] - 2r_B^2 - \frac{1}{2}\pi r_B^2}{\pi r^2}\right]^N\right]}{r^2} dx. \quad (4)$$

Integrating (4), we arrive at the final result in the closed-form of (5), where the shortcuts are

$$A = \frac{(h_B - h_{Rx})}{h_{Tx} - h_{Rx}}, \quad B = 2r_B^2 - \frac{\pi r_B^2}{2}. \quad (6)$$

### 3.1.2. D2D Scenario

Since the heights of Tx and Rx are assumed to be equal,  $h_{Tx} = h_{Rx} < h_B$ , it suffices to consider a two-dimensional case, whose top view is shown in Fig. 2(b). Given the distance  $x$  between Tx and Rx, the area of the LoS blockage zone is given by

$$S_B(x) = 2r_B x - 4r_B^2 - \pi r_B^2. \quad (7)$$

Similarly to the AP blockage model, there is no blockage when Tx and Rx are closer than  $4r_B$ . Recalling the stationary property of RDM model and the fact that the distance between two points uniformly distributed in the circle of radius  $\pi r^2$  is given by [27] as

$$f(x) = \frac{2x}{r^2} \left[ \frac{2 \arccos\left(\frac{x}{2r}\right)}{\pi} - \frac{x \sqrt{1 - \frac{x^2}{4r^2}}}{r\pi} \right], \quad x \in (0, 2r), \quad (8)$$

we have the following for the fraction of LoS

$$p_L = 1 - \int_{4r_B}^r f(x) \left[1 - \left[1 - \frac{2r_B x - 4r_B^2 - \pi r_B^2}{\pi r^2}\right]^N\right] dx, \quad (9)$$

that coincides with the LoS blockage probability. Note, the integral cannot be expressed in elementary functions but can be computed numerically for an arbitrary set of input parameters.

### 3.1.3. PPP Deployment of APs and Multi-connectivity

The abovementioned results can also be obtained for PPP deployment of APs and blockers moving according to RDM with intensities  $\lambda_A$  and  $\lambda_B$ , respectively. In this case, the distance between UE moving according to RDM model and the nearest AP coincides with the distance between APs in PPP. The pdf of distance to  $i$ -s neighbor in the Poisson field of APs is [27] as

$$f_i(x) = \frac{2(\pi\lambda)^i}{(i-1)!} x^{2i-1} e^{-\pi\lambda x^2}, \quad x > 0, \quad i = 1, 2, \dots \quad (10)$$

We introduce the area of the LoS blockage zone similarly to (2) and observe that there exists the LoS path if there are no blockers currently in this zone. Since random translation of the blockers PPP according to RDM is still PPP the LoS probability coincides with the void probability of PPP [28]. Thus, the LoS probability with the nearest AP is given by

$$p_{L,1} = 1 - e^{\int_0^\infty (2r_B[x - d(x)] - 2r_B^2 - \frac{1}{2}\pi r_B^2) f_1(x) dx}, \quad (11)$$

that can be numerically estimated.

Using the similar approach one may obtain probability of LoS with  $i$ -s nearest AP,  $p_{L,i}$ . If UE simultaneously supports  $K$  connections to  $i$  nearest APs, the LoS probability can be approximated by

$$p_L = 1 - \prod_{i=1}^K (1 - p_{L,i}). \quad (12)$$

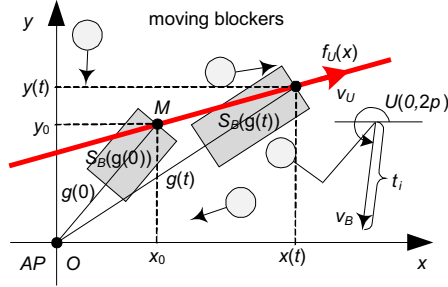
### 3.2. Blockage and Non-Blockage Intervals

We now proceed characterizing LoS blockage and non-blockage intervals. As the principal difference between AP and D2D scenarios is in the length of the LoS blockage zone, in what follows, we address the AP scenario only.

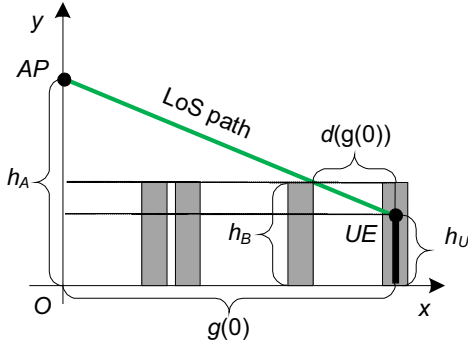
We approach the problem as follows. First, we introduce the movement trajectory. Then, we proceed with specifying a Markov model for a randomly chosen instant of time  $t$ . Without the loss of generality, we have chosen  $t = 0$ . We then consequentially define the area of the LoS blockage zone, the intensity of blockers entering it and the mean duration of blocked and non-blocked intervals. These latter quantities allow formulating an approximating Markov model of the blockage process. Finally, we extend this model to time-dependent behavior incorporating previously defined movement trajectory.

Embed the coordinate system such that the position of AP is at  $O$ , see Fig. 3(a) and let  $w_U(x) = ax + b$  the trajectory of a moving UE. Let UE be at  $(x_0, y_0)$  such that  $w_U(x_0) = ax_0 + b$  at time instant  $t = 0$ . Let  $g(t)$  be the function specifying the distance to the AP at time  $t$ .

$$p_L = \frac{\left[ \frac{r(2(A-1)r_B + \pi r) + B}{r^2} \right]^{N+1} [r(\pi r - 2(A-1)(N+1)r_B) + B]}{2\pi^N (A-1)^2 (N+1)(N+2)r_B^2} - \frac{4r_B^2}{r^2} - \frac{\left[ \frac{4(A-1)r_B^2 + B + \pi r^2}{r^2} \right]^{N+1} [\pi r^2 - 4(A-1)(N+1)r_B^2 + B]}{2\pi^N (A-1)^2 (N+1)(N+2)r_B^2}. \quad (5)$$



(a) Top view



(b) Side view

Figure 3: LoS blockage with mobile blockers and AP.

Since at time  $t = 0$  UE is at  $(x_0, y_0)$  and given a certain speed of UE,  $v_U$ , the coordinates of UE time  $t$  are

$$\begin{cases} x(t) = x_0 + v_U t \cos a, \\ y(t) = y_0 + v_U t \sin a, \end{cases} \quad (13)$$

leading to the distance to AP at  $t$

$$g(t) = \sqrt{(x_0 + v_U t \cos a)^2 + (y_0 + v_U t \sin a)^2}. \quad (14)$$

Consider the process of LoS blockage by a dynamically moving blockers around the stationary user of interest at  $t = 0$  and an AP located at the distance  $g(x_0)$  from the UE. Similarly to the previous section, we identify the LoS blockage zone as shown in Fig. 3. The LoS blockage zone can be approximated by a rectangle with area

$$S_B(g(t)) = 2r_B \left( g(t) \frac{h_B - h_U}{h_A - h_U} + r_B \right). \quad (15)$$

To characterize the dynamics of the blockage process in zone  $i$ , we first consider the intensity of blockers arrivals,

$\gamma(x)$ , to the LoS blockage zone. Extending the results of [29], the inter-meeting time of a single blocker with the LoS blockage zone is exponential with parameter

$$\begin{aligned} \gamma_1(g(0)) &= v S_B(g(0)) \iint_W f^2(s) ds = \\ &= v E S_B(g(0)) \int_0^{2\pi} d\phi \int_{r_{i-1}}^{r_i} \frac{1}{\pi R^2} dr = \frac{2v_B S_B(g(0))}{\pi R^3}, \end{aligned} \quad (16)$$

where  $W$  is the coverage area of AP,  $v_B$  is the speed of a moving blocker, and  $f(s) = 1/\pi R^2$  is the stationary distribution of the RDM [26].

As the number of blockers in AP coverage area is Poisson with intensity of  $\lambda_B \pi R^2$ , the process of blockers occluding the LoS path is Poisson with the intensity

$$\gamma(g(0)) = \frac{2v_B \lambda_B S_B(g(0))}{R}. \quad (17)$$

Following [29], the process of blockers entering LoS blockage zone is Poisson with parameter  $\gamma(g(0))$ . Due to the properties of RDM model, the entrance point of a blocker is uniformly distributed over three sides of the LoS blockage zone. Also, the process of blocked and non-blocked periods forms an the alternative renewal process [30]. Let  $\Theta(g(0))$  and  $\Omega(g(0))$  be the RVs denoting the blocked and non-blocked periods respectively. Since the blockers enter the zone according to a Poisson process with the intensity  $\gamma(g(0))$ , the time spent in the unblocked part,  $\Omega(g(0))$ , is exponentially distributed,  $F_\Omega(\tau; g(0)) = 1 - e^{-\gamma(g(0))\tau}$  [30] with mean

$$E[\Omega(g(t))] = \frac{R}{2v_B \lambda_B S_B(g(t))}, \quad (18)$$

that can be verified by observing that the left-hand sides of the individual blockers entering the blockage zone follow a Poisson process. Hence, the distance from the end of the blocked part, considered as an arbitrary point, to the starting point of the next blocked interval is exponential.

The mean blockage time can be found using the fraction of time the UE is not blocked,  $p_L$ . Recalling that the flow in and flow out of the AP coverage zone are assumed to be equal, the distribution of the number of blockers in the coverage zone of AP is Poisson. Using the void probability of the Poisson process, we have [28]

$$p_L(g(0)) = \exp[-\lambda_B S_B(g(0))]. \quad (19)$$

Using the property of the renewal process [30], we write

$$p_L(g(0)) = \frac{E[\Omega(g(0))]}{E[\Theta(g(0))] + E[\Omega(g(0))]}, \quad (20)$$

immediately leading to

$$E[\Theta(g(t))] = \frac{Re^{-\lambda_B S_B(g(t))}}{2\lambda_B v_B S_B(g(t))[1 - e^{-\lambda_B S_B(g(t))}]}, \quad (21)$$

where we substituted  $p_L(g(0))$  and  $E[\Omega(g(0))]$ .

The movement of UE does not change the structure of the blockage process but affect the form of blockage and non-blockage durations distributions. To characterize the dynamics of the blockage process, we approximate the blockage process at the time  $t = 0$  using a continuous-time Markov chain (CTMC) with two states and the following infinitesimal generator

$$\Lambda(g(0)) = \begin{bmatrix} -\alpha(g(0)) & \alpha(g(0)) \\ \beta(g(0)) & -\beta(g(0)) \end{bmatrix}, \quad (22)$$

where  $\alpha(g(0)) = 1/E[\Theta(g(0))]$ ,  $\beta(g(0)) = 1/E[\Omega(g(0))]$  are the mean durations of blocked and non-blocked intervals. Note that this model is approximate in nature as the duration of the blockage period follows general distribution, as shown in [22].

To enable UE movement, we allow transition rates to vary in time. Using previously obtained results, the time-dependent intensities take the following form

$$\begin{cases} \alpha(g(t)) = \frac{2\lambda_B v_B S_B(g(t))[1 - e^{-\lambda_B S_B(g(t))}]}{Re^{-\lambda_B S_B(g(t))}}, \\ \beta(g(t)) = \frac{2\lambda_B v_B S_B(g(t))}{R}. \end{cases} \quad (23)$$

#### 4. Extensions of the Baseline Model

The baseline model allows for a number of extensions. Aside from the straightforward one to the case of more complex UE trajectories, there are few principal extensions. In this section, we address the following: (i) multi-connectivity option of 3GPP NR technology, (ii) mobility of AP, and (iii) random AP deployment.

##### 4.1. Multi-Connectivity

The blockage of LoS path between UE and AP may lead to the outage. Simultaneous support of multiple connections with NR APs, known as multi-connectivity, is considered as a way to reduce the number and duration of outage events [15, 16].

As an example, consider the blockage process with two APs, shown in Fig. 4(a). The associated CTMC model is given by superposition of CTMCs modeling the blockage processes with individual APs. Letting  $g_i(t)$ ,  $i = 1, 2$  to denote the distance to the first and second APs at time  $t$ , the infinitesimal generator takes the following form

$$\Lambda_i = \begin{bmatrix} -\sum \alpha(g_1(t)) & \alpha(g_1(t)) & 0 \\ \beta(g_2(t)) & -\sum 0 & \alpha(g_1(t)) \\ \beta(g_1(t)) & 0 & -\sum \alpha(g_2(t)) \\ 0 & \beta(g_1(t)) & \beta(g_2(t)) & -\sum \end{bmatrix}, \quad (24)$$

where  $\alpha(g_i(t))$ ,  $\beta(g_i(t))$  are the rates of the blockage process with AP  $i$ , state 1 corresponds to the blockage state, and  $\sum$  sign denotes the sum of all row elements.

The extension to more than two APs is straightforward.

##### 4.2. Mobile AP

Recently, several authors have proposed to use mobile AP to improve the network capacity on-demand in places where there is a spontaneous need for more capacity at the air interface. One such option is to use unmanned aerial vehicles (UAV), such as drones [31, 32]. UAV-based NR AP can be mobile when providing service to UE inducing three-sides mobility that can also be captured using the proposed model.

Assuming that the trajectory of AP is known and can be represented by  $w_A(x) = cx + d$ , the only extension needed to construct the CTMC modeling of the blockage process is to determine the time-dependent distance between AP and UE. Aligning  $OX$  with the direction of AP movement and assuming that the distance between AP and UE at time  $t_0$  is  $g(0) = \sqrt{x_0^2 - y_0^2}$ , we see that the distance between AP and UE at time  $t$  from Fig. 4(b), obeys

$$g(t) = \sqrt{(x_0 + \cos av_U t)^2 + (y_0 + \sin av_U t - v_A t)^2}, \quad (25)$$

and the rest of the procedure is similar to the baseline.

##### 4.3. Random APs Deployment

It has been shown that positions APs may not be deterministic [33, 34]. The proposed model can be extended to the case of random AP deployments as sketched below.

Let  $G$  be a RV denoting the distance between AP and UE at time  $t_0$  and let  $f_G(x)$ ,  $x > 0$ , be its pdf. The probability of LoS at  $t_0$  is then

$$p_L(g(0)) = \int_0^\infty f_G(x) e^{-\lambda_B S_B(g(0))} dx. \quad (26)$$

Recall that for each fixed distance  $x$  from AP to UE, the LoS duration is exponentially distributed with parameter  $\gamma(g(0))$ . Thus, the mean LoS period is given by

$$E[\Omega(x; t_0)] = \int_0^\infty f_G(x) \frac{1}{\gamma(g(0))} dx, \quad (27)$$

while the mean blockage period is calculated using (21) completing parameterization of the CTMC model.

To enable the movement of the UE, we need to calculate the distance between UE and AP at time  $t > 0$ . This can be done using (25), where the coordinates  $(x_0, y_0)$  are now a function of RV  $G$ ,  $X_0 = G \cos a$ ,  $Y_0 = G \sin a$  leading to the following random functions specifying the distance between AP and UE at time  $t$

$$\begin{cases} X(t) = \cos a(G + v_U t), \\ Y(t) = \sin a(G + v_U t), \end{cases} \quad (28)$$

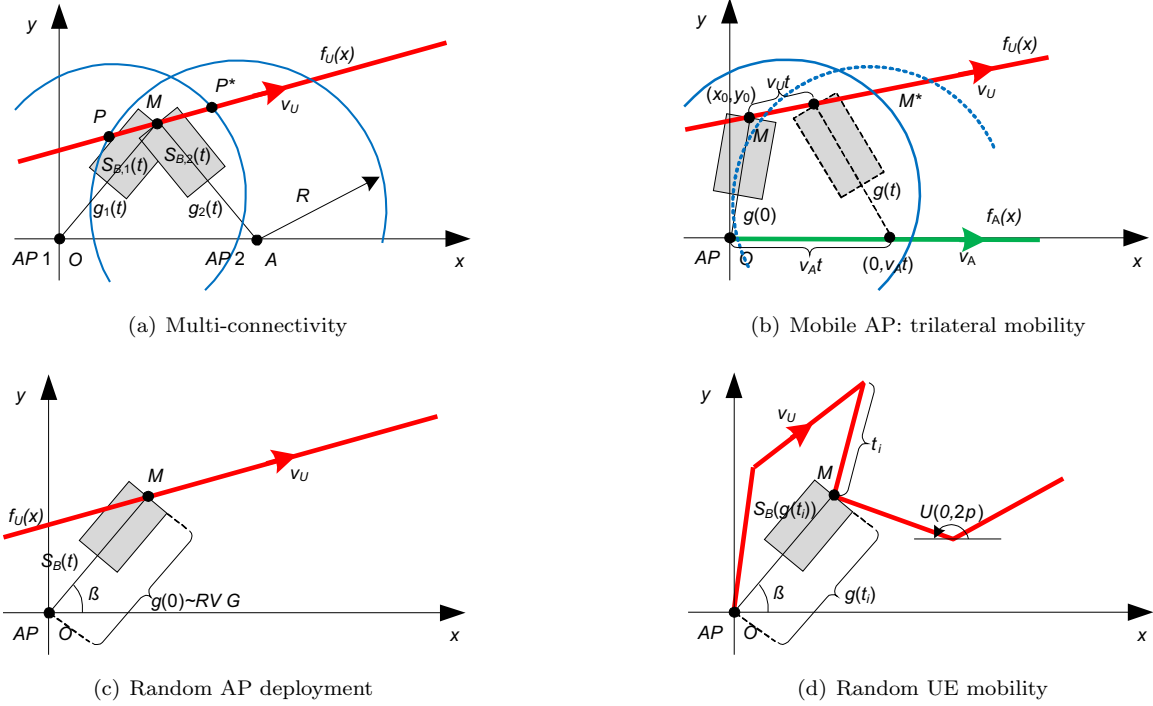


Figure 4: Illustrations of the baseline model feasible extensions.

resulting in the following distance to AP at time  $t$

$$G(x; t) = \sqrt{[\cos a(x + v_U t)]^2 + \sin^2 a(x + v_U t)}, \quad (29)$$

where  $x$  follows RV  $G$ , and  $t$  is the parameter.

Thus, the pdf of the distance at time  $t$  can be estimated using non-linear transformation of RV [35]. Recall that pdf of a RV  $G(t)$ ,  $f_G(y; t)$ , expressed as a function  $y = g(x; t)$  of another RV  $G$  with pdf  $f_G(x)$ , is [36]

$$f_G(y; t) = \sum_{\forall i} f_G(\psi(y)) |\psi'(y)|, \quad (30)$$

where  $x = \psi(y) = g^{-1}(x; t)$  is the inverse function.

Considering the popular homogeneous PPP model of AP locations with intensity of  $\theta$ , the distance to the nearest AP is provided by [27]

$$f_G(x) = 2\pi\theta x e^{-\pi\theta x^2}, \quad x > 0. \quad (31)$$

The inverse of the positive branch of  $g(x; t)$  and the modulo of its derivative are given by

$$\psi(y) = \frac{\sec^4 a \sqrt{\cos^4 a (4x^2 \cos^2 a + C - \cos(2a) + 1)}}{2},$$

$$|\psi'(y)| = \frac{8\sqrt{2}x \sin^2(a) \cos^2(a) + 8x \cos^2(a)}{4\sqrt{\cos^4 a (4x^2 \cos^2 a + C - \cos(2a) + 1)}}, \quad (32)$$

where the shortcut  $C$  is

$$C = \sqrt{2 \sin^2 a (8x^2 \cos^2 a - \cos(2a) + 1)}, \quad (33)$$

leading to the pdf of  $G(t)$  in closed-form of (34).

Now, the time-dependent LoS probability, and mean durations of LoS blockage and non-blockage periods can be calculated using (26) and (27).

The extension to the multi-connectivity case is straightforward since the distance to the  $i^{\text{th}}$  nearest neighbor in PPP is available in closed-form [27]. We specifically note that once UE moves along its trajectory, the nearest AP may change. Recall that the part of the plane where a specific AP is nearest to the UE is given by Voronoi tessellation of  $\mathfrak{R}^2$  [28]. Voronoi tessellation of  $i$ -s order can be applied to define the plane partitioning to the cells where each point of a UE trajectory is closer to  $i$ -s APs.

Note that additional elements of uncertainty can be brought to the model assuming, e.g., random speeds of UE and AP. In this case, (29) becomes a function of multiple RVs. Nevertheless, the distribution of  $G(y; t)$  can still be found using RV transformation technique [35].

#### 4.4. Random UE Mobility

In some environments, e.g., parks or walking streets, the mobility of UE may not be deterministic but is better described by some random mobility process. The extension of the baseline model to this case can be performed for a limited set of mobility processes having closed-form distribution of the distance between a fixed point and a randomly moving one. In what follows, we consider one such process, a modified RDM model with constant flight lengths, known as Pearson-Rayleigh walk [37].

Let  $(0, 0)$  be the coordinates of UE at time  $t = 0$ , that is UE starts at origin, where AP is located. It has been

$$f_G(y; t) = \frac{1}{4}\pi\theta \sec^4 a \left( \frac{8\sqrt{2}x \sin^2 a \cos^2 a}{C} + 8y \cos^2 a \right) \exp \left( -\frac{1}{4}\pi\theta \sec^4(a) (4y^2 \cos^2 a + C - \cos(2a) + 1) \right), y > 0. \quad (34)$$

shown in [38] that the joint pdf of the distance from a point moving according to Pearson-Rayleigh random walk to the origin at the step  $i$ , conditioned on the traveled time  $t_i = l_i/v_u$  is

$$f_i(x|t_i) = \begin{cases} \frac{1}{2\pi t_i} \delta \left( t_i - \frac{r}{v_U} \right), & i = 1 \\ \frac{i}{2\pi t_i^2} \left( 1 - \frac{x^2}{t_i^2} \right)^{\frac{m-2}{2}}, & i = 2, 3, \dots \end{cases} \quad (35)$$

where  $\delta(\cdot)$  is the Kronecker delta function,  $r$  is the length of a single step.

Since the transition rates of the blockage process depend on the distance between AP and UE, we can now parameterize CTMC model at the stopping times of the Pearson-Rayleigh model similarly to the previous subsection. Owing to the straight movement direction between stopping times  $t_i$  the transition rates at times  $t \in (t_i, t_{i+1})$  between stopping times can be linearly approximated.

Using recent results for RDM mobility model and specifying the distance between two points moving according to RDM processes, we can further extend the baseline model to the case of randomly moving AP [39].

## 5. Applications and Time-Dependent Behavior

### 5.1. System Level Simulations

Although the considered CTMC is non-homogeneous, it can be easily used in simulation studies based on well-known methods for simulations of non-stationary Poisson processes, see, e.g., [40, 41]. Particularly, assume that the chain just entered the LoS state at time  $t_0 = 0$ . The CCDF of time until the blockage periods starts again is available in closed-form (36), where the coefficients are

$$\begin{aligned} A &= \sqrt{2ab(tv_U + x_0) + (a+1)^2(tv_U + x_0)^2 + b^2}, \\ B &= 4\lambda_B r_B v_B \left( \frac{h_B - h_U}{h_A - h_U} + r_B \right), \\ C &= \sqrt{2abx_0 + (a+1)^2x_0^2 + b^2}. \end{aligned} \quad (37)$$

Note that although no generic expression is available for CCDF of the blockage period,  $F_B(t)$ ,  $t > 0$ , it can be obtained in closed-form for a particular UE trajectory. For example, assuming UE trajectory coinciding with the  $OX$  axis, we arrive at

$$\begin{aligned} F_B(t) &= D - \frac{x_0 \left( \frac{F(0,0)G(0,0)}{E} - x \right)}{2v_U x_0} + \\ &+ \frac{\sqrt{(tv_U + x_0)^2} \left[ \frac{F(t, v_U)G(t, v_U)}{E} - t^2 v_u^2 - 2tv_U x_0 - x_0^2 \right]}{2v_U (tv_U + x_0)}, \end{aligned} \quad (38)$$

where the coefficients are

$$\begin{aligned} D &= \frac{4\lambda_B r_B v_B [h_A r_B + h_B - h_U (r_B + 1)]}{R(h_A - h_U)}, \\ E &= 2\pi^2 \lambda_B^2 R^4 r_B^2 [h_A r_B + h_B - h_U (r_B + 1)]^2, \\ F(x, y) &= (h_A - h_U) e^{\frac{2\pi \lambda_B R^2 r_B \sqrt{xy + x_0^2} (h_A r_B + h_B - h_U (r_B + 1))}{h_A - h_U}}, \\ G(x, y) &= \frac{2\pi \lambda_B R^2 r_B \sqrt{xy + x_0^2}}{(h_U r_B + h_U - h_A r_B - h_B)^{-1}} + h_A + h_U. \end{aligned} \quad (39)$$

### 5.2. Analytical Studies of 3GPP NR Technology

The developed CTMC model also allows for advanced applications in analytical studies of NR technologies. This is facilitated by the explicit closed-form structure of the transition rates  $\alpha(t)$  and  $\beta(t)$ . Below, we obtain several metrics of interest for the baseline model including (i) SNR and rate process dynamics, (ii) state probability at time  $t$ ,  $p_i(t)$ , (iii) fraction of time in blockage, and (iv) distribution and mean time to outage.

#### 5.2.1. SNR and Rate Processes Dynamics

The blockage process does not provide valuable information for system designers. The reason is that blockage itself does not imply that UE is in outage conditions as NR link may still be established using alternative propagation paths. The time-dependent structure of the proposed modeling framework allows to specify the time-dependent propagation, signal-to-noise ratio (SNR), and capacity processes as UE moves using the framework of Markov modulated processes. For example, assuming  $B$  Hz of allocated resources, the time-dependent capacity is

$$C(t) = cB \log[1 + S(t)], t > 0, \quad (40)$$

where  $S(t)$  is the SNR at time  $t$ ,  $c$  is a constant accounting for imperfections of the modulation and coding schemes (MCS).  $S(t)$ , measured in dB, is expressed as a function of system parameters and the blockage process,

$$S(t) = \frac{P_T G_T G_R}{P_L(t) N_F(B)}, t > 0, \quad (41)$$

where  $P_T$  is the transmit power,  $G_T$  and  $G_R$  are the transmit and receive antenna gains,  $N_F$  is the noise level at bandwidth  $B$ ,  $P_L(t)$  is the only time-dependent component.  $P_L(t)$  depends on (i) the distance to AP at time  $t$ ,  $g(t)$ , and (ii) the propagation model. Thus, using appropriate propagation model, e.g., standardized 3GPP [12] or simplified Nokia model [42], one can associate each state of CTMC with the rate function  $R_i(t)$ ,  $i = 1, 2$  that explicitly accounts for performance degradation caused by dynamic

$$F_L(t) = \frac{(a+1)A(a((a+2)(tv_U + x_0) + b) + tv_U + x_0) + (2a+1)b^2 \log(aA + A + ab + (a+1)^2(tv_U + x_0))}{2(a+1)^3 v_U R B^{-1}} - \frac{(a+1)(ab + (a+1)^2 x_0)C + (2a+1)b^2 \log(a(C + (a+2)x_0 + b) + C + x_0)}{2(a+1)^3 v_U R B^{-1}}, \quad t > 0. \quad (36)$$

blockage. When multi-connectivity of degree  $K > 1$  is considered, each state is associated with the rate function  $R_i = \max_{\forall j} R_{i,j}$ , where  $j$  is the index of AP.

### 5.2.2. State Probability at Time $t$ , $p_i(t)$

Let  $p_i(t)$  time-dependent probabilities that the system is in the state  $i$  at time  $t$ ,  $p_i(t)$ . For CTMC blockage model the latter satisfies the following system [36]

$$\begin{cases} \frac{dp_1(t)}{dt} = p_2(t)\beta_1(t) - p_1(t)\alpha_1(t), \\ \frac{dp_2(t)}{dt} = p_1(t)\alpha_1(t) - p_2(t)\beta_1(t), \end{cases} \quad (42)$$

with the normalizing condition  $p_2(t) = 1 - p_1(t)$ ,  $t > 0$ .

The general solution of the linear differential equation with time-varying coefficients and initial condition  $p_1(0) = 1$  is provided in [43]

$$p_1(t) = \exp \left[ - \int_0^t [\alpha(\tau) + \beta(\tau)] d\tau \right] \times \left[ \int_0^t \beta(\tau) \exp \left[ \int_0^\tau [\alpha(x) + \beta(x)] dx \right] d\tau + 1 \right], \quad (43)$$

that can be solved for any particular UE trajectory.

When multi-connectivity of degree  $K > 2$  is considered, one needs to solve the system of  $2^{K-1}$  non-linear differential equations with time-varying coefficients. This can be done using the method of parameters variations for any realistic value of  $K$  [43].

### 5.2.3. Fraction of Time in Blockage

One of the applications of time-dependent blockage probability is finding the fraction of time in blockage for a given UE trajectory. Assuming that UE is at the distance  $g(0)$  at time  $y = 0$ , it can be done by a direct integration of  $p_1(t)$  as follows

$$f_B = \int_0^T p_1(t) dt, \quad (44)$$

that can be estimated for a particular UE trajectory.

### 5.2.4. Time to Outage

Generally, the outage could be defined as the event when SNR falls below a certain SNR threshold,  $S_O$  [44].  $S_O$  is often determined as the lowest value of SNR that can be used for reliable communications between AP and UE, i.e., there is still MCS that can maintain the required

block error probability. Note that blockage does not always lead to an outage. However, using the NR propagation model [42, 12], we can specify a circular area around AP,  $R_O$  where the loss of LoS does not lead to an outage.

Let the UE at  $t = 0$  be at the egress point from the circle with radius  $R_O$ , defined by the intersection of  $x^2 + y^2 - R_O^2 = 0$  and  $y - ax - b = 0$ , with coordinates

$$\begin{cases} x_0 = \frac{-\sqrt{a^2 R_O^2 - b^2 + R} \pm ab}{a^2 + 1}, \\ y_0 = -\frac{\pm a \sqrt{a^2 R_O^2 - b^2 + R}}{a^2 + 1} - \frac{a^2 b}{a^2 + 1} + b. \end{cases} \quad (45)$$

Let  $f_O(t)$ ,  $t > 0$ , be the pdf of the time to outage. Observe that at the egress point UE can be in blocked or non-blocked state. The blockage state probability is  $1 - p_L(g(0))$ , see (19). The outage is immediately experienced and the mass at zero is  $f_O(0) = 1 - p_L(g(0))$ . Alternatively, the time to outage with the current AP is the first passage time (FPT) of CTMC to the blocked state conditioned that the model is in non-blocked state at  $t = 0$ . Let  $f_{O|\neq 1}(t)$  be the pdf of FPT from the set of non-blocking states,  $\{2, 3, \dots, 2^K\}$  to the blockage state 1, where  $K$  is the degree of multi-connectivity. The sought distribution is of phase-type [45] with representation  $(\vec{\rho}, S)$ , where  $\vec{\rho}$  is the initial state distribution at  $t = 0$  defined over  $\{2, 3, \dots, 2^K\}$ , and  $S$  is the rate matrix obtained from  $\Lambda_i$  in (24) excluding the first row and column. The conditional pdf is then given by

$$f_{O|\neq 1}(t) = \vec{\rho} e^{St} \vec{s}_0, \quad t > 0, \quad (46)$$

where  $\vec{s}_0 = -S\vec{1}$ ,  $\vec{1}$  is the vector of ones of size  $1 \times 2^K - 1$ ,  $e^{St}$  is the matrix exponential.

The initial state probability vector  $\rho$  can be found from the steady-state distribution,  $\vec{\pi}$  of the time-homogeneous CTMC blockage model of stationary UE at time  $t = 0$  which is the solution of the system  $\vec{\rho}\Lambda_i = \vec{\rho}$ ,  $\rho\vec{e} = 1$ , where  $\vec{e}$  is the unit vector. Particularly, we arrive at

$$\rho_i = \frac{\pi_i}{1 - p_L(g(0))}, \quad i = 1, 2, \dots \quad (47)$$

## 6. Numerical Analysis

In this section, we numerically illustrate the proposed methodology by providing results for specific system deployments. We consider examples related to the following cases: (i) closed zone of interest with a finite number of blockers for AP and D2D scenario, and (ii) random deployments of APs in  $\mathfrak{R}^2$ . Particularly, in Subsection 6.1,

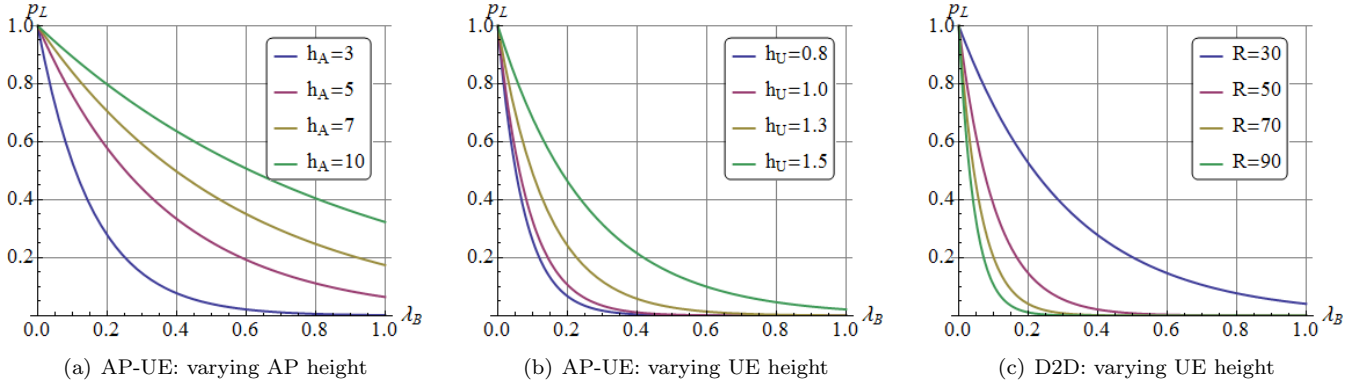


Figure 5: Fraction of LoS time in various considered scenarios.

we start addressing the fraction of time in blockage for both AP-UE and D2D scenarios for a closed zone of interest. Then, we turn the attention to the PPP deployment and proceed with characterizing the local behavior of the process considering time-series of the blockage process in Subsection 6.2. The mean blockage and non-blockage intervals as a function of system parameters for PPP deployment is analyzed in Subsection 6.3.

The main input parameters for both closed zone and PPP deployments are summarized in Table 6. Unless explicitly specified, these parameters are assumed to be used for numerical examples.

Table 2: Default parameters for numerical assessment.

Parameter	Value
Height of AP, $h_A$	4 m
Height of blockers, $h_B$	1.7 m
Height of UE, $h_U$	1.5 m
Blocker radius, $r_B$	0.4 m
Speed of blockers, $v_B$	1 m/s
Speed of UEs, $v_U$	1 m/s
AP intensity, $\lambda_A$	0.001 AP/m <sup>2</sup>
Blockers intensity, $\lambda_B$	0.1 bl/m <sup>2</sup>
AP coverage radius, $R$	100 m
D2D zone radius, $R$	100 m

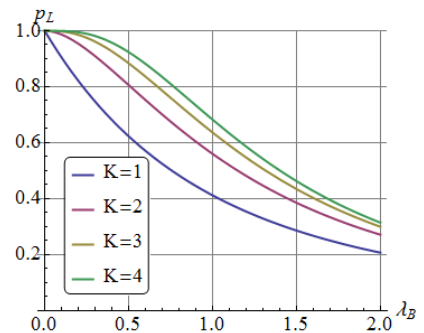
### 6.1. Time-Averaged Characterization

We first concentrate on time-averaged metric – a fraction of LoS time, which is analyzed in Subsection 3.1 for AP-UE and D2D scenarios, see (5) and (9). Note that below we use  $\lambda_B$  to denote intensity of blockers in a zone of interest. The actual number of blockers is given by  $\pi R^2 \lambda_B$ , where  $R$  is the radius of closed zone of interest.

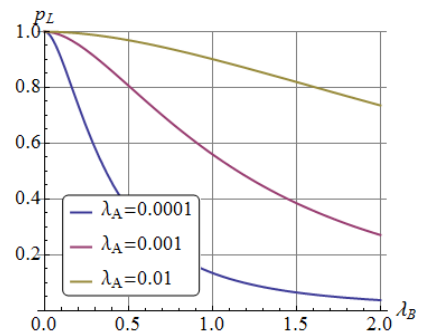
Consider first the AP to UE communications scenario. Fig. 5(a) and Fig. 5(b) illustrate the fraction of LoS time as a function of systems parameters including AP height,  $h_A$ , and UE height,  $h_U$ , respectively. Expectedly, as the number of blockers increases the probability of LoS fraction decreases exponentially. The height of both UE and

AP significantly affects the fraction of time in LoS state. However, the effect of AP height is much more profound. Particularly, for  $\lambda_B = 0.4$  increasing the AP height from 3 to 10 meters allows improving the fraction of LoS from around 0.5 to approximately 0.65. Thus, the AP height is one of the critical parameters to improve NR systems performance in relatively crowded places.

The effect of input parameters on the fraction of LoS blockage time for the D2D scenario is illustrated in Fig. 5(c) as the function of the blockers intensity for different radii of the service area. Recall that in this scenario, the height of communicating entities is the same and equal to 1.5 m while the height of blockers is 1.7 m. Logically, the frac-



(a) Varying degree of multiconnectivity



(b) Varying intensity of APs

Figure 6: Effect of multiconnectivity on fraction of LoS time.

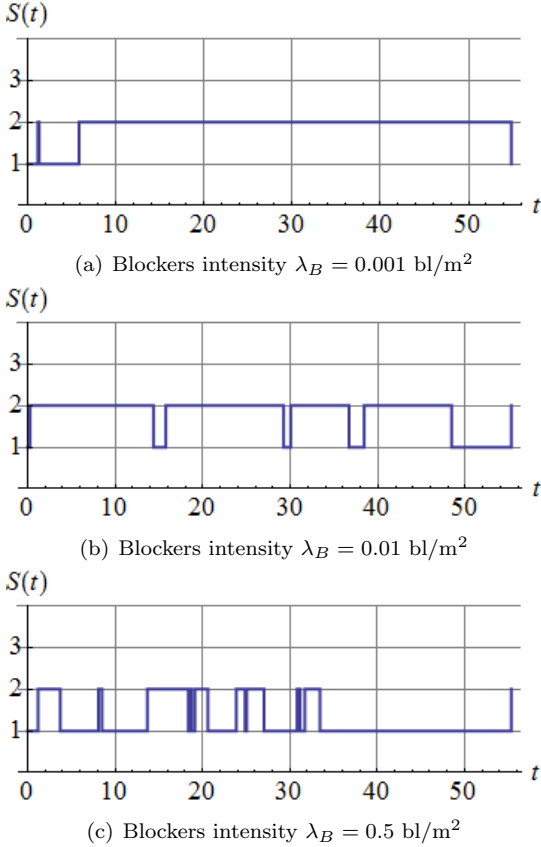


Figure 7: Time-series of model for different blockers intensity.

tion of LoS blockage time increases as the distance between communicating entities increases by keeping the number of blockers constant and increasing the service area of interest. By comparing the results in Fig. 5(c) with Fig. 5(a), and 5(b), we observe that the fraction of the LoS time for the D2D scenario is significantly lower. Indeed, since the heights of communicating entities are the same, the area of the LoS blockage zone is larger.

Next, for PPP deployment of APs and blockers in  $\mathcal{R}^2$  with intensities  $\lambda_A$  and  $\lambda_B$ , respectively, we concentrate on the effect of multi-connectivity on the fraction of time at least one AP is not blocked. Here, the UE, as well as blockers, are assumed to move in  $\mathcal{R}^2$  according to RDM. Fig. 6 shows the probability that at least one AP out of  $K$  nearest is in non-blocked conditions. Analyzing the data in Fig. 6(a), one may notice that the major improvement stems from adding a single backup link, that is, maintaining active links to two nearest APs. When  $K$  increases further additional gains are visible, but they diminish as  $K$  grows. Thus, Fig. 6(b) shows the response of the metric for different intensities of AP in  $\mathcal{R}^2$ . Here, increasing the density of AP has a hugely positive effect on the probability that at least one AP out of two nearest is in non-blockage conditions that, indeed, makes multi-connectivity an attractive option for future dense deployments of NR cellular systems.

## 6.2. Local Characteristics of the Blockage Process

Time-averaged metrics, such as a fraction of time in LoS state, do not entirely characterize performance experienced by moving UE in a field of blockers. Indeed, several applications may tolerate abrupt rate drops and even outages caused by blockage by implementing application layer bufferization or rate adaptation. Thus, it is critical to understand the local response of the blockage process to system metrics of interest. We are particularly interested in time-series of the model and mean durations of the blocked and non-blocked periods.

To illustrate time series of the model, consider the scenario, where UE moves according to RDM in  $\mathcal{R}^2$  in a PPP field of blockers and APs of intensities  $\lambda_B$  and  $\lambda_A$ . The results demonstrated below have been obtained using computer simulation of the Markov model specified in Subsection 3.2 and extended to the case of multi-connectivity in Section 4. The time-series of the model for different intensities of blockers in the environment and the blockers and UE velocity is set to  $v_B = v_U = 1$  m/s, shown in Fig. 7. Here, state 1 corresponds to the blocked state while state 2 to the non-blocked state. The increase in the density of blockers profoundly affects the time spend in the blocked state. Furthermore,  $\lambda_B = 0.5$  results in blocked periods of exceptionally large durations for high blockers intensity.

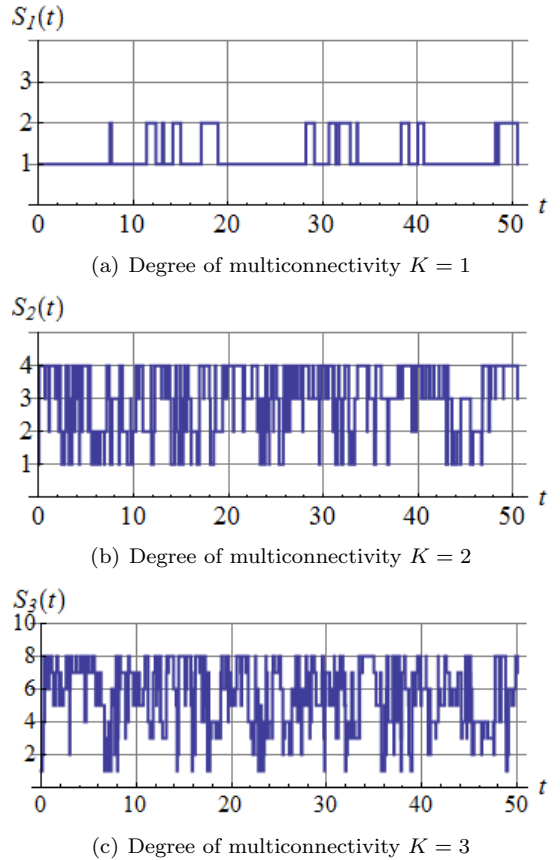


Figure 8: Time-series for different degrees of multiconnectivity.

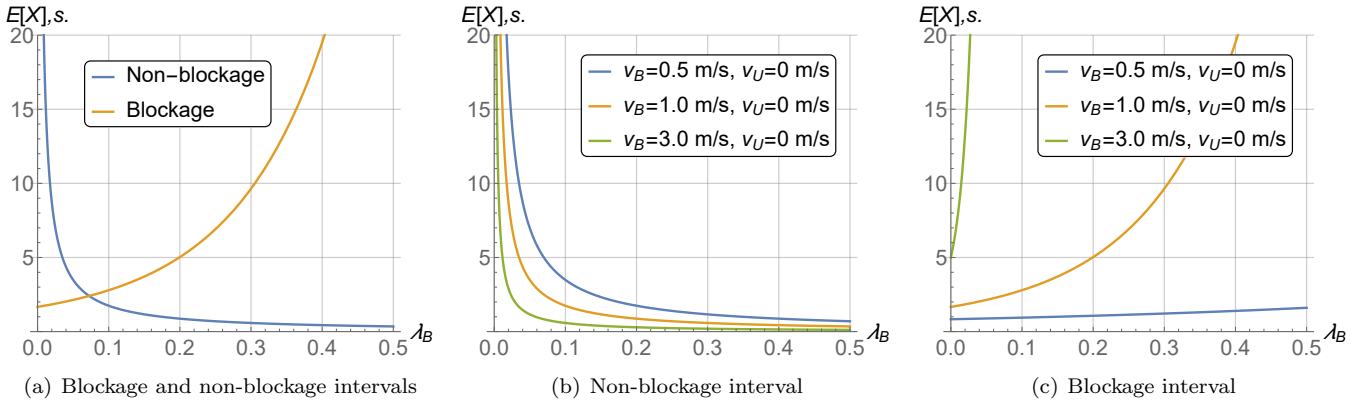


Figure 9: Means of blockage and non-blockage time intervals.

Consider now the effect of multi-connectivity on local behavior of the blockage process. Fig. 8 shows the time-series of the blockage process for different degrees of multi-connectivity and  $\lambda_B = 1$ . Here, state 1 corresponds to the case when LoS paths to all available APs are simultaneously blocked. Any other state implies there is at least one non-blocked LoS path. As one may observe, the use of two APs allows to reduce the time UE spends in blocked conditions drastically. Adding one more link by increasing the degree of multi-connectivity to  $K = 3$  allows improving the performance even further. However, this effect is milder compared to the increase from one to two simultaneously supported links.

### 6.3. Means of Blocked and Non-Blocked Intervals

Time-series observations provide intuition on the qualitative effects of the system parameters on local behavior of the blockage process. Below, we complement this knowledge with a quantitative analysis demonstrating the means of blockage and non-blockage intervals. The results reported below are obtained in Subsection 3.2.

Fig. 9 shows means of blockage and non-blockage intervals as a function of blockers intensity for different speeds of blockers,  $v_B$ . First, the mean blockage interval increases as the intensity of blockers increases, as depicted in Fig. 9(a). The trend for the mean non-blockage interval is reverse. It is essential that the mean non-blockage interval decreases at a much higher rate compared to the increase in the mean blockage interval. Then, when  $\lambda_B$  increases even further, the durations of non-blockage intervals drastically decreases while blockage intervals become long-lasting.

Fig. 9(b) and Fig. 9(c) show the effect of blockers speed,  $v_B$ , on mean durations of blockage and non-blockage intervals. As one may expect, the response of these metrics to the blockers speed is straightforward. Particularly, higher values of  $v_B$  lead to shorter duration of the non-blockage periods and longer duration of the blockage intervals. The magnitude of this effect is non-linear and heavily depends on  $\lambda_B$ . Note that the effect of UE speed is similar and, thus, not reported here.

We note that for realistic values of pedestrian speeds, the mean duration of the blockage period is on the order of a fraction of a second. This implies that applications that do not rely on buffering (e.g., real-time streaming) will experience a significant degradation in service performance. Applications utilizing buffering may adaptively choose the duration of the prefetching period depending on the blockers intensity as well as speeds of UE and blockers.

## 7. Conclusions

Inspired by the need for efficient modeling approaches of the propagation paths blockage process in 3GPP NR systems operating in the mmWave frequency band, we have developed a simple yet accurate model for LoS blockage process that accounts for mobility of both UE and blockers in this paper. Particularly, we first characterized the LoS blockage process in two representative scenarios deriving the fractions of time LoS is blocked as well as the duration of the blockage and non-blockage intervals. We then formulated a simple Markov chain model capturing the dynamics of the LoS blockage process. The baseline model allows for a number of extensions including (i) AP mobility, (ii) random AP deployment, and (iii) 3GPP multi-connectivity operation.

The applications scope of the proposed model includes both system level simulations and analytical analysis of 3GPP NR systems. Specifically, the developed Markov model can be efficiently used in simulations, where it can abstract the process of the propagation paths blockage that is known to affect the computational complexity significantly. The model is also suitable for analytical studies of 3GPP NR deployments providing a simple yet accurate description of the LoS blockage process. In particular, we have demonstrated how the model can be used to determine the following quantities: (i) SNR and capacity process dynamics, (ii) probability that at time  $t$  the system is at the blockage or non-blockage state, (iii) fraction of time in blockage and (iv) mean and distribution of time to outage.

## References

## References

- [1] J. Du, E. Onaran, D. Chizhik, S. Venkatesan, and R. A. Valenzuela, "Gbps User Rates Using mmWave Relayed Backhaul With High-Gain Antennas," *IEEE Journal on Selected Areas in Communications*, vol. 35, no. 6, pp. 1363–1372, 2017.
- [2] S. Andreev, V. Petrov, M. Dohler, and H. Yanikomeroglu, "Future of Ultra-Dense Networks Beyond 5G: Harnessing Heterogeneous Moving Cells," *arXiv preprint arXiv:1706.05197*, 2017.
- [3] A. Vizziello, P. Savazzi, and K. R. Chowdhury, "A Kalman based Hybrid Precoding for Multi-User Millimeter Wave MIMO Systems," *IEEE Access*, 2018.
- [4] V. Petrov, A. Pyattaev, D. Moltchanov, and Y. Koucheryavy, "Terahertz band communications: Applications, research challenges, and standardization activities," in *Proc. of 8th International Congress on Ultra Modern Telecommunications and Control Systems and Workshops (ICUMT)*, pp. 183–190, IEEE, 2016.
- [5] V. Petrov, J. Kokkonen, D. Moltchanov, J. Lehtomäki, M. Juntti, and Y. Koucheryavy, "The Impact of Interference from the Side Lanes on mmWave/THz Band V2V Communication Systems with Directional Antennas," *IEEE Transactions on Vehicular Technology*, vol. 67, no. 6, pp. 5028–5041, 2018.
- [6] R. Kovalchukov, D. Moltchanov, A. Samuylov, A. Ometov, S. Andreev, Y. Koucheryavy, and K. Samouylov, "Analyzing Effects of Directionality and Random Heights in Drone-based mmWave Communication," *IEEE Transactions on Vehicular Technology*, 2018.
- [7] D. Moltchanov, A. Samuylov, V. Petrov, M. Gapeyenko, N. Himayat, S. Andreev, and Y. Koucheryavy, "Improving Session Continuity with Bandwidth Reservation in mmWave Communications," *IEEE Wireless Communications Letters*, 2018.
- [8] K. Zeman, M. Stusek, J. Pokorny, P. Masek, J. Hosek, S. Andreev, P. Dvorak, and R. Josth, "Emerging 5G Applications over mmWave: Hands-on Assessment of WiGig Radios," in *Proc. of 40th International Conference on Telecommunications and Signal Processing (TSP)*, pp. 86–90, IEEE, 2017.
- [9] Solomitckii D., et. al., "Comparative Evaluation of Radio Propagation Properties at 15 GHz and 60 GHz Frequencies," in *Proc. of 9th International Congress on Ultra Modern Telecommunications and Control Systems and Workshops (ICUMT)*, pp. 91–95, IEEE, 2017.
- [10] V. Ishakian, I. Matta, and J. Akinwumi, "On the Cost of Supporting Mobility and Multihoming," in *Proc. of GLOBECOM Workshops (GC Wkshps)*, pp. 310–314, IEEE, 2010.
- [11] K. Yang, A. Pellegrini, M. Munoz, A. Brizzi, A. Alomainy, and Y. Hao, "Numerical Analysis and Characterisation of THz Propagation Channel for Body-Centric Nano-Communications," *IEEE Tran. on THz Science and Tech.*, vol. 5, pp. 419–426, May 2015.
- [12] 3GPP, "Channel Model for Frequency Spectrum above 6 GHz (Release 14)," 3GPP TR 38.900 V2.0.0, 2016.
- [13] S. Deng, M. Samimi, and T. Rappaport, "28GHz and 73GHz Millimeter-Wave Indoor Propagation Measurements and Path Loss Models," in *Proc. IEEE ICC*, 2015.
- [14] G. MacCartney, J. Zhang, S. Nie, and T. Rappaport, "Path loss models for 5G millimeter wave propagation channels in urban microcells," in *Proc. IEEE GLOBECOM*, pp. 3948–3953, Dec. 2013.
- [15] V. Petrov, D. Solomitckii, A. Samuylov, M. A. Lema, M. Gapeyenko, D. Moltchanov, S. Andreev, V. Naumov, K. Samouylov, M. Dohler, et al., "Dynamic Multi-connectivity Performance in Ultra-dense Urban mmWave Deployments," *IEEE Journal on Selected Areas in Communications*, vol. 35, no. 9, pp. 2038–2055, 2017.
- [16] M. Polese, M. Giordani, M. Mezzavilla, S. Rangan, and M. Zorzi, "Improved Handover through Dual Connectivity in 5G mmWave Mobile Networks," *IEEE Journal on Selected Areas in Communications*, vol. 35, no. 9, pp. 2069–2084, 2017.
- [17] D. Moltchanov, A. Ometov, S. Andreev, and Y. Koucheryavy, "Upper Bound on Capacity of 5G mmWave Cellular with Multi-connectivity Capabilities," *Electronics Letters*, vol. 54, no. 11, pp. 724–726, 2018.
- [18] M. Gapeyenko, et. al., "Analysis of Human Body Blockage in Millimeter-Wave Wireless Communications Systems," in *Proc. of International Conference on Communications (ICC)*, IEEE, May 2016.
- [19] T. Bai, R. Vaze, and R. W. Heath Jr., "Analysis of Blockage Effects on Urban Cellular Networks," *IEEE Transactions on Wireless Communications*, pp. 5070–5083, Sept. 2014.
- [20] "Evolved Universal Terrestrial Radio Access (E-UTRA); Further advancements for E-UTRA physical layer aspects (Release 9)," *3GPP TR 36.814 V9.0.0*, March 2010.
- [21] A. Samuylov, M. Gapeyenko, D. Moltchanov, M. Gerasimenko, S. Singh, N. Himayat, S. Andreev, and Y. Koucheryavy, "Characterizing Spatial Correlation of Blockage Statistics in Urban mmWave Systems," in *Proc. of Globecom Workshops (GC Wkshps)*, pp. 1–7, IEEE, 2016.
- [22] M. Gapeyenko, A. Samuylov, M. Gerasimenko, D. Moltchanov, S. Singh, M. R. Akdeniz, E. Aryafar, N. Himayat, S. Andreev, and Y. Koucheryavy, "On the Temporal Effects of Mobile Blockers in Urban Millimeter-Wave Cellular Scenarios," *arXiv preprint arXiv:1705.08037*, 2017.
- [23] A. Trotta, M. Di Felice, F. Montori, K. R. Chowdhury, and L. Bononi, "Joint Coverage, Connectivity, and Charging Strategies for Distributed UAV Networks," *IEEE Transactions on Robotics*, vol. 34, no. 4, pp. 883–900, 2018.
- [24] A. Trotta, F. D. Andreagiovanni, M. Di Felice, E. Natalizio, and K. R. Chowdhury, "When UAVs Ride A Bus: Towards Energy-efficient City-scale Video Surveillance," in *Proc. of IEEE Conference on Computer Communications (INFOCOM)*, pp. 1043–1051, IEEE, 2018.
- [25] D. Moltchanov and A. Ometov, "On the Fraction of LoS Blockage Time in mmWave Systems with Mobile Users and Blockers," in *International Conference on Wired/Wireless Internet Communication*, pp. 183–192, Springer, 2018.
- [26] P. Nain, D. Towsley, B. Liu, and Z. Liu, "Properties of Random Direction Models," in *Proc. of 24th Annual Joint Conference of the IEEE Computer and Communications Societies*, vol. 3, pp. 1897–1907, IEEE, 2005.
- [27] D. Moltchanov, "Distance Distributions in Random Networks," *Elsevier Ad Hoc Networks*, vol. 10, pp. 1146–1166, Aug. 2012.
- [28] S. Chiu, D. Stoyan, W. Kendall, and J. Mecke, *Stochastic geometry and its applications*. Wiley, 2013.
- [29] R. Groenevelt, "Stochastic Models for Mobile Ad Hoc Networks," PdD thesis, INRIA Sophia-Antipolis, 2005.
- [30] D. R. Cox, *Renewal theory*. Methuen and Co Ltd., 1970.
- [31] S. Sekander, H. Tabassum, and E. Hossain, "Multi-tier drone architecture for 5G/B5G cellular networks: Challenges, trends, and prospects," *IEEE Communications Magazine*, vol. 56, no. 3, pp. 96–103, 2018.
- [32] A. Orsino, A. Ometov, G. Fodor, D. Moltchanov, L. Militano, S. Andreev, O. N. Yilmaz, T. Tirronen, J. Torsner, G. Araniti, et al., "Effects of Heterogeneous Mobility on D2D-and Drone-Assisted Mission-Critical MTC in 5G," *IEEE Communications Magazine*, vol. 55, no. 2, pp. 79–87, 2017.
- [33] Y. Li, F. Baccelli, H. S. Dhillon, and J. G. Andrews, "Fitting Determinantal Point Processes to Macro Base Station Deployments," in *Proc. of Global Communications Conference (GLOBECOM)*, pp. 3641–3646, IEEE, 2014.
- [34] S. Zhou, D. Lee, B. Leng, X. Zhou, H. Zhang, and Z. Niu, "On the Spatial Distribution of Base Stations and its Relation to the Traffic Density in Cellular Networks," *IEEE Access*, vol. 3, pp. 998–1010, 2015.
- [35] S. Ross, *Introduction to probability models*. Academic Press, 2010.
- [36] W. Feller, *An introduction to probability theory and its applications*, vol. 1. Wiley, 3rd ed., 1968.
- [37] G. Le Caër, "A Pearson Random Walk with Steps of Uniform Orientation and Dirichlet Distributed Lengths," *Journal of Sta-*

- tistical Physics*, vol. 140, no. 4, pp. 728–751, 2010.
- [38] M. Franceschetti, “When a Random Walk of Fixed Length Can Lead Uniformly Anywhere Inside a Hypersphere,” *Journal of Statistical Physics*, vol. 127, no. 4, pp. 813–823, 2007.
- [39] A. D. Kolesnik, “Probability Law for the Euclidean Distance Between Two Planar Random Flights,” *Journal of Statistical Physics*, vol. 154, no. 4, pp. 1124–1152, 2014.
- [40] P. A. Lewis and G. S. Shedler, “Simulation Methods for Poisson Processes in Nonstationary Systems,” in *Proc. of 10th conference on Winter simulation*, pp. 155–163, IEEE Press, 1978.
- [41] N. Ma and W. Whitt, “Efficient Simulation of non-Poisson non-Stationary Point Processes to Study Queueing Approximations,” *Statistics & Probability Letters*, vol. 109, pp. 202–207, 2016.
- [42] T. A. Thomas, H. C. Nguyen, G. R. MacCartney, and T. S. Rappaport, “3D mmWave Channel Model Proposal,” in *Proc. of 80th Vehicular Technology Conference (VTC Fall)*, pp. 1–6, IEEE, 2014.
- [43] J. K. Hale, “Functional Differential Equations,” in *Analytic theory of differential equations*, pp. 9–22, Springer, 1971.
- [44] J. G. Proakis, *Companders*. Wiley Online Library, 2001.
- [45] T. Altiok, “On the Phase-type Approximations of General Distributions,” *IIE Transactions*, vol. 17, no. 2, pp. 110–116, 1985.